First-principle study on optical properties of N–La-codoped anatase TiO*

Wang Qing(王 青)[a)†], Liang Ji-Feng(梁纪锋)[a)], Zhang Ren-Hui(张仁辉)[b)], Li Qiang(李 强)[c)], and Dai Jian-Feng(戴剑锋)[a)]

[a)] School of Science, Lanzhou University of Technology, Lanzhou 730050, China
[b)] State Key Laboratory of Solid Lubrication, Lanzhou Institute of Chemical Physics, Chinese Academy of Sciences, Lanzhou 730000, China
[c)] Sichuan Provincial Key Laboratory of Computational Physics, Yibin University, Yibin 644000, China

(Received 11 July 2012; revised manuscript received 12 December 2012)

The electronic structures, deformation charge density, dipole moment, and optical properties of N–La-codoped anatase titanium dioxide (TiO_2) are studied using the plane-wave ultrasoft pseudopotential method based on the density functional theory (DFT). The optical properties of two-ion-doped TiO_2 are analyzed via electronic structures, deformation charge density, and dipole moment. For the model of N–La-doped TiO_2, a smaller atom fraction of N and La atoms induces better optical properties. The absorption edges of two doped TiO_2 models redshift to the visible-light region.

Keywords: optical property, first-principle study, electronic structure, deformation charge density

PACS: 78.20.Bh, 71.15.Mb, 78.40.Fy, 71.15.−m **DOI:** 10.1088/1674-1056/22/5/057801

1. Introduction

Nowadays, energy shortage and water pollution are two important issues in the world, which we urgently need to solve. Anatase titanium dioxide (TiO_2) has been used in solar cells, purification of water and air, and photolysis of water and optical degradation of organic compounds, due to its unique optical, electrical, and chemical properties. However, as a wide-band gap oxide semiconductor ($E_g = 3.23$ eV), anatase TiO_2 only shows photocatalytic activity under UV-light irradiation that accounts for only a small fraction of the solar energy,[1,2] so its utilization of solar energy is very low.[3,4] Furthermore, its photo quantum yield value is also very low due to its photoexcited electron-hole pairs easily recombining. Recently, many attempts have been made to improve the photocatalytic activity of TiO_2 under visible-light irradiation, such as transition metal and nonmetal doping,[5–8] lanthanides doping,[9,10] semiconductor compounding,[11] and organic dye sensitizing.[12–14] In these attempts, ion doping is considered one of the most efficient methods. Zhao *et al.*[15] found that addition of nitrogen and vanadium can effectively make the fundamental absorption edge of TiO_2 red-shift. Asahi *et al.*[16] believed that the N-2p states and the O-2p states are hybridized in N-doped TiO_2, leading to a narrower energy band gap of TiO_2 and subsequently visible light absorption. However, Irie *et al.*[17] suggested isolated N-2p states above the valence-band maximum of TiO_2, which is consistent with several recent experimental studies.[18–21] Dai *et al.*[22] reported that N-2p states lie in the band gap of TiO_2, and the mixing of N-2p states with O-2p states is too weak to produce a significant band-gap narrowing. Lin *et al.*[23] found that the photocatalytic activities of La_2O_3- or Y_2O_3-doped anatase TiO_2 were much better than pure TiO_2. Jing *et al.*[24] reported that La-doped TiO_2 exhibits a good photocatalytic performance. Clearly, these researchers have mainly focused on the single-ion doping into TiO_2. Up to now, the influence of multiple-ion codoping into TiO_2 on the photocatalytic performance was mostly studied in experiments.[25–29] However, different experimental conditions and sample preparation methods made it difficult to understand their intrinsic mechanism. Alternatively, computer simulation can overcome the complexity of experimental conditions, and help us analyze the microscopic information of electronic structure and band structure of the doped TiO_2 and understand how the different doped elements and doped position impact photocatalytic activity of TiO_2 under visible-light irradiation.[30,31]

Thus, in the present work, the electronic structure, deformation charge density, dipole moment, and optical properties of N–La-codoped anatase TiO_2 are studied using the plane-wave ultrasoft pseudopotential method based on the density functional theory (DFT).

2. Models and calculation methods

The two doped TiO_2 models are displayed in Figs. 1(a) and 1(b). As shown in Fig. 1(a), one O atom is replaced by one N atom, and one Ti atom is replaced by one La atom ($2 \times 1 \times 1$ super cell). The atom concentration of impurity is about 8.34% (atom fraction) in total. In Fig. 1(b), two O atoms are substituted by N atoms and one Ti atom is replaced by one La atom

*Project supported by the National Natural Science Foundation of China (Grant No. 50873047).
†Corresponding author. E-mail: wangqing@lut.cn
© 2013 Chinese Physical Society and IOP Publishing Ltd

($2 \times 1 \times 1$ super cell). The atom concentration of impurity is about 12.51% (atom fraction) in total.

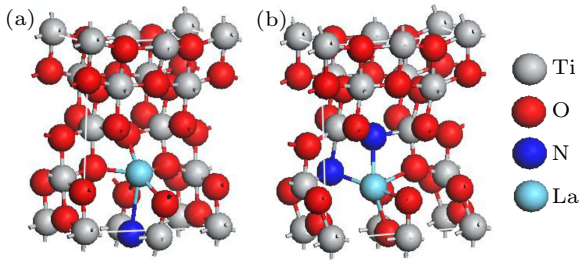


Fig. 1. (color online) (a) Model of N–La-codoped anatase TiO_2; (b) model of 2N–La-codoped anatase TiO_2.

All calculations are performed with the CASTEP module of Materials Studio 5.0.[32] The ultrasoft pseudopotential is used in the calculation because of its several advantages in efficiency and veracity in the reciprocal space. The electronic exchange-correlation energy is treated within the framework of the generalized gradient approximation (GGA) with PW91 function.[33] The plan-wave expansion is truncated by the cutoff energy of 360 eV. The Monkhorst–Park scheme K-point grid sampling is set as $3 \times 3 \times 3$ for the models (a) and (b). Mulliken population analysis is used to analyze the average net charge. The Mulliken population is defined as the electronic charge assigned to the atoms, atomic orbitals, and chemical bonds. The wave function is obtained using the molecular orbital theory, and it is transformed into a visual chemical information in this method. Then, the transfer of electrons in molecules, molecular polarity, and the type and strength of chemical bonds are studied using this method. In order to ensure the comparability of results, the real space sample is divided into 0.04 nm $\times$ 0.04 nm $\times$ 0.03 nm for all models. The convergence value is set as 2.0×10^{-3} nm for the maximum displacement tolerances, 0.05 eV/nm for the maximum force, 0.1 GPa for the maximum stress, and 1.0×10^{-5} eV per atom for the total energy change in the geometrical optimization.[5,10] The crystal structures and atom's coordinates are also optimized firstly under the principle of energy minimization to obtain the appropriate cell parameters, so that we could obtain stable structures for all the models.[15] Based on this principle, the electronic structures and optical properties could be calculated. After geometrical optimization, the lattice parameters of the pure anatase TiO_2 are given as follows: $a = b = 3.7973$ Å, $c = 9.7851$ Å. These parameters are well consistent with the experimental values, $a = b = 3.7848$ Å, $c = 9.5124$ Å,[34] which indicates that the calculation methods are reasonable and the calculation results should be reliable.

2.1. Dipole moments

Optical properties of a semiconductor are mostly dependent on its electronic structures. The change of the electronic structures can make the center of gravity of negative electric deviate from the position in the super cell, and results in non-zero dipole moments.[35] Therefore, studying the relationship between dipole moment and optical properties would help us understand how to improve the visible-light absorption of the TiO_2. Sato *et al.*[36] reported that the local internal fields due to the dipole moment of the distorted octahedral can promote the charge separation in the initial process of photoexcitation and are useful for enhancing photocatalytic activity. Considering that much research has focused on the calculation of the octahedral dipole moment but not the total of dipole moment within a super cell in the past,[15] the dipole moments of all elements in the super cell were calculated in this work. The average net charges calculated using the Mulliken population analysis are shown in Table 1. With these results, the center of gravity of six O ions in TiO_6 octahedron and the distance between the center of O ion and Ti ion can be calculated. Finally, the TiO_6dipole moment will be obtained by using the dipole moment formula ($\mu = qr$, where q is the net charge, and r is the distance between the center of O ion and Ti ion).[37]

In the situation that N and La atoms are codoped into anatase TiO_2, there are some significant changes in the local electronic density. When an O atom is replaced by an N or La atom, the charge distribution of the system is correspondingly changed, so the electrons of higher electronic density can easily obtain smaller energy and enter into a lower energy region when the holes are left in their original positions.

The dipole moment of a distorted octahedron can induce the local internal fields which are beneficial to the separation of photoexcited electrons and holes and are useful for enhancing photocatalytic activity.[38] In our recent investigation, it is found that a larger dipole moment of TiO_6 octahedron causes higher absorption coefficient in the visible-light region, as shown in Table 1.

Table 1. Formation energies, average bond lengths, average net charges, average dipole moments and absorption coefficient of deficient iondoped TiO_2 by geometry optimization.

	Bond length/Å			Net charge/eV				Dipole moment/D	Absorption coefficient
	Ti-O	Ti-N	La-O	Ti	O	N	La	TiO_6	at $\lambda = 450$ nm/cm^{-1}
Pure TiO2	1.9326[36]	–	–	1.270[36]	−0.630[36]	–	–	0.000[36]	0
N–La-doped	1.9325	2.1195	2.5323	1.144	−0.656	−0.540	2.290	0.1932	3.34×10^4
2N–La-doped	2.0018	2.2622	2.4670	1.147	−0.670	−0.450	2.450	0.1661	2.16×10^4

2.2. Electronic structure and optical properties

The band structure, density of states, and deformation charge density of N–La-doped and 2N–La-doped anatase TiO_2 on the aforementioned geometric configurations are displayed in Figs. 2, 3, and 4, respectively. From Figs. 2(a) and 2(b), it can be observed that there are two impurity energy levels of N-2p state, and the impurity energy levels are split. Obviously, the optical electrons gain energy to induce the transition of electrons from the valence band into the conduction band. As a result, the absorption coefficient decreases in the visible-light region. As shown in Fig. 3, it is found that the figures of density of states are consistent with the analysis of band structures.

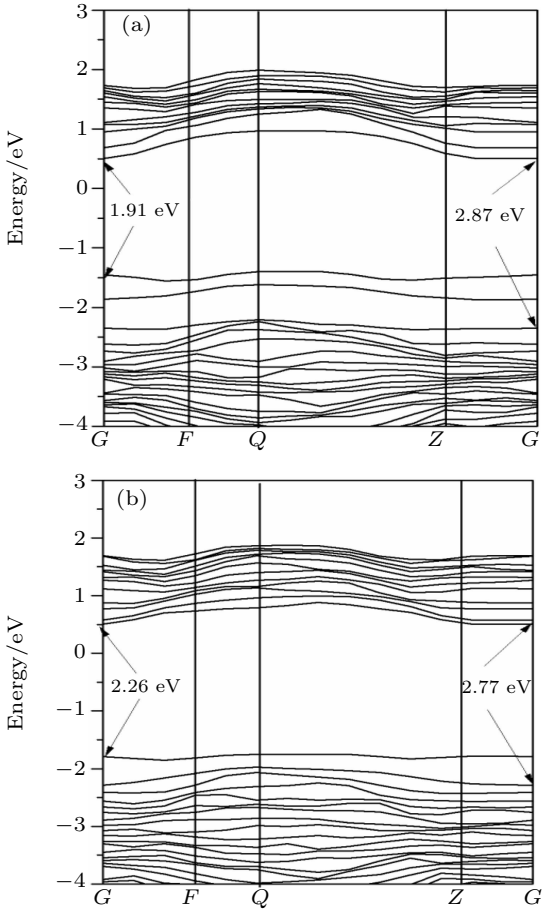


Fig. 2. Band structures of (a) N–La-doped anatase TiO_2, and (b) 2N–La-doped anatase TiO_2.

The band structures and density of states are obviously different in two models because of the different positions of the doped atoms. The locations of N and La atoms in the N–La-codoped TiO_2 also affect the electronic structure of TiO_2. The charge of N atom is −0.540 eV and the charge of La atom is 2.290 eV in model (a). While the charge of N atom is −0.450 eV and the charge of La atom is 2.450 eV in model (b). The band lengths of La–O and Ti–N are 2.5323 Å and 2.1195 Å in model (a), and 2.4670 Å and 2.2622 Å in model (b), respectively. From Figs. 2 and 4, it can be observed that a large lattice distortion occurs in models (a) and (b). Generally speaking, a small lattice distortion can be helpful for increasing the dipole moment. Moreover, enhancing the optical absorption in the visible-light region, N–La-doped TiO_2 (Fig. 4(b)) leads to the electronic charge density redistribution. The O atoms originally bonded with Ti atoms are drawn to bond with the La atom. The dipole moment of TiO_6 octahedron is the largest among the two models. In the visible-light region, the absorption coefficient is also the highest among the two models. In Fig. 4(c), the electron clouds mainly distribute between the bonding axis of N atom and Ti atom, and there are a few electron clouds between the O atom and La atom. The dipole moment of TiO_6 octahedron is 0.1661 D.

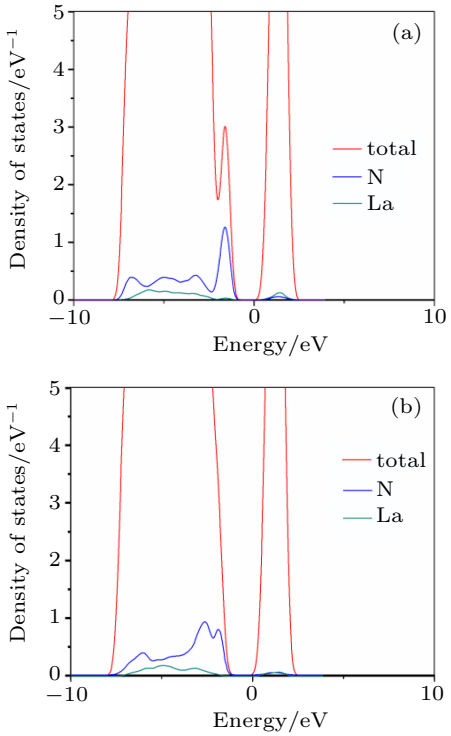


Fig. 3. (color online) Density of states for (a) N–La-doped anatase TiO_2, and (b) 2N–La-doped anatase TiO_2.

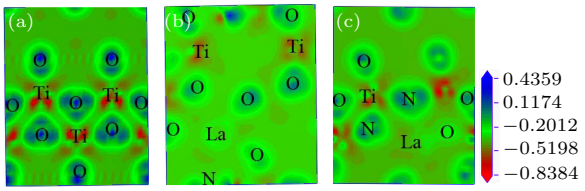


Fig. 4. (color online) Deformation charge density of (a) pure anatase TiO_2, (b) N–La-doped anatase TiO_2, and (c) 2N–La-doped anatase TiO_2.

On the basis of the electronic structure, the optical absorption spectra of pure polycrystalline anatase TiO_2 and two doped models between 250 nm and 1100 nm are calculated, and the results are shown in Fig. 5. It is found that the calculated values of optical absorption of N–La-doped TiO_2 agree well with the experimental values in Ref. [39]. For these calculations, the scissors operator applied is 0.60 eV, accounting for

the difference between the experimental band gap (3.23 eV) and the calculated band gap. From Fig. 5, compared with pure TiO_2, the fundamental absorption edge red-shifts toward visible-light region.

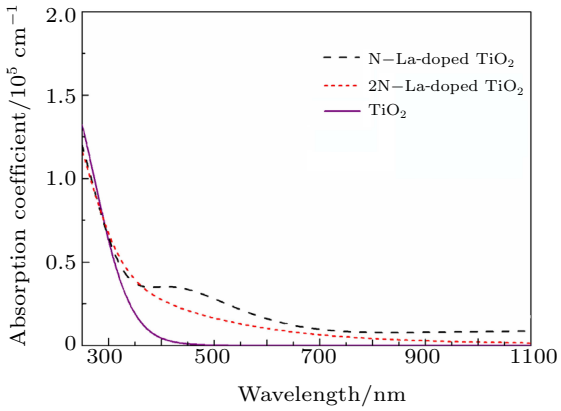


Fig. 5. (color online) Calculated optical absorption curves of pure TiO_2 and two ion-doped anatase TiO_2.

3. Conclusions

In summary, two optimized models of N–La-doped TiO_2 are proposed, and their optical properties are simulated in this work. The results show that the calculated values of visible-light absorption of 2N–La-doped TiO_2 (model (b)) are consistent with the experimental values. The visible-light absorption edge obviously red-shifts in both models. In general, the large dipole moment in the super cell can enhance the optical responses of the visible light for doped TiO_2. The optical properties of model (a) (atom fraction: 8.34%) is better than that of model (b) (atom fraction: 12.51%), suggesting that the atom fraction of N and La atom in N–La-doped TiO_2 model has a significant influence on the optical properties of doped TiO_2. The visible-light absorption of N–La-doped TiO_2 could be further improved through controlling the distance between La and O atoms, increasing the dipole moment of the super cell and decreasing the fraction of the doped atoms.

References

[1] Wang B L and Hu L L 2004 *Chin. Phys.* **13** 1887
[2] Li C Y, Wang J B and Wang Y Q 2012 *Chin. Phys. B* **21** 098102
[3] Gole J L, Stout J D, Burda C, Lou Y B and Chen X B 2004 *J. Phys. Chem. B* **4** 108
[4] Zhang T H, Piao L Y, Zhao S L, Xu Z, Wu Q and Kong C 2012 *Chin. Phys. B* **21** 118401
[5] Zhang X C, Zhao L J, Fan C M, Liang Z H and Han P D 2012 *Physica B* **407** 4416
[6] Anpo M, Takeuchi M, kimura T, Hidaka M and Rakhmawaty D 2007 *J. Catal.* **246** 235
[7] Cheng L, Gan Z H, Liu W and Zhao X Z 2012 *Acta Phys. Sin.* **61** 237107 (in Chinese)
[8] Gao P, Wu J, Liu Q J and Zhou W F 2010 *Chin. Phys. B* **19** 087103
[9] Chen W G, Yuan P F, Zhang S, Sun Q, Liang E J and Jia Y 2012 *Physica B* **407** 1038
[10] Li C, Hou Q Y, Zhang Z D, Zhao C W and Zhang B 2012 *Acta Phys. Sin.* **61** 167103 (in Chinese)
[11] Fujii H, Inata K, Ohtaki M, Eguchi K and Arai H 2001 *J. Mater. Sci.* **36** 527
[12] Otaka H, Kira M, Yano K, Ito S, Mitekura H, Kawata T and Matsui F 2004 *J. Photochem. Photobiol. A* **164** 67
[13] Xiong B T, Zhou B X, Bai J, Zheng Q, Liu Y B, Cai W M and Cai J 2008 *Chin. Phys. B* **17** 3713
[14] Hong X G, Du L C, Ye M P and Weng Y X 2004 *Chin. Phys.* **13** 720
[15] Zhao Z Y and Liu Q 2008 *J. Catal. Lett.* **124** 111
[16] Asahi R, Morikawa T, Ohwaki T, Aoki K and Taga Y 2001 *Science* **293** 269
[17] Irie H, Watanabe Y and Hashimoto K 2003 *J. Phys. Chem. B* **107** 5483
[18] Lindgren T, Mwabora J M, Avendano E, Jonsson J, Hoel A, Granqvist C G and Lindquist S E 2003 *J. Phys. Chem. B* **107** 5709
[19] Torres G R, Lindgren T, Lu J, Granqvist C G and Lindquist S E 2004 *J. Phys. Chem. B* **108** 5995
[20] Nakamura R, Tanaka T and Nakato Y 2004 *J. Phys. Chem. B* **108** 10617
[21] Lee J Y, Park J and Cho J H 2005 *Appl. Phys. Lett.* **87** 11904
[22] Dai S J, Hu C W and Du L 2008 *Acta Chim. Sin.* **66** 1620 (in Chinese)
[23] Lin J and Yu J C 1998 *J. Photochem. Photobiol. A* **116** 63
[24] Jing L Q, Sun X J, Xin B F, Wang B Q, Cai W M and Fu H G 2004 *J. Solid State Chem.* **177** 3375
[25] Xu X H, Tian Y and Wu J F 2008 *J. Wuhan Univ. Technol.* **30** 543 (in Chinese)
[26] Liu P, Li R P and Dong H C 2008 *Chin. Rare Earth.* **29** 5 (in Chinese)
[27] Ding P, Liu F M, Zhou C C, Zhong W W, Zhang H, Cai L G and Zeng L G 2010 *Chin. Phys. B* **19** 118102
[28] Yan Z Y, Zhang D K, Miao H, Shang Y B, Yang J, Ye Y X, Hu X Y, Liu E Z and Fan J 2011 *Chin. Phys. B* **20** 087803
[29] Li G H, Wu Y C and Zhang L D 2001 *Chin. Phys.* **10** 148
[30] Gong S and Liu B G 2012 *Chin. Phys. B* **21** 057104
[31] Chen Q and Cao H H 2004 *Chin. Phys.* **13** 2121
[32] Segall M D, Lindan P J D, Probert M J, Pickard C J, Hasnip P J, Clark S J and Payne M C 2002 *J. Phys.: Condens. Matter* **14** 2717
[33] Lu Z H, Ma D W, Zhang J, Xu G L and Yang Z X 2012 *Chin. Phys. B* **21** 047505
[34] Jeremy K B, Timothy H and Gordon J M 1987 *J. Am. Chem. Soc.* **109** 3639
[35] Zhang R H, Wang Q, Liang J, Li Q, Dai J F and Li W X 2011 *Physica B* **407** 2709
[36] Sato J, Kobayashi H and Inoue Y 2003 *J. Phys. Chem. B* **107** 7970
[37] Gao P, Zhang X J, Zhou W F, Wu J and Liu Q J 2010 *J. Semicond.* **31** 032001
[38] Sato J, Kobayashi H, Ikarashi K, Saito N, Nishiyama H and Inoue Y 2004 *J. Phys. Chem. B* **108** 4369
[39] Wei H Y, Wu Y S, Lun N and Zhao F 2004 *J. Mater. Sci.* **39** 1305